Identification of miR-20a as A Potential Discerning Biomarker for Non-Invasive versus Invasive Retinoblastoma

Ahmad Bereimipour, M.Sc.[1, 2], Saeed Karimi, M.D.[3]* (iD), Mohammad Faranoush, M.D.[4], Amir-Abbas Hedayati Asl,

M.D.[1], Monireh-sadat Miri, M.Sc.[1], Leila Satarian, Ph.D.[1]* (iD), Sara Taleahmad, Ph.D.[1]* (iD)

1. Department of Stem Cells and Developmental Biology, Cell Science Research Center, Royan Institute for Stem Cell Biology and Technology, ACECR, Tehran, Iran
2. Faculty of Sciences and Advanced Technologies in Biology, University of Science and Culture, Tehran, Iran
3. Ophthalmology Department, Eye Research Center, Shahid Beheshti University of Medical Sciences, Tehran, Iran
4. Pediatric Growth and Development Research Center, Institute of Endocrinology and Metabolism; MAHAK Pediatric Cancer Treatment and Research Center, Iran University of Medical Sciences, Tehran, Iran

Abstract

Objective: Intraocular retinoblastoma (RB) is common in kids. Although the cause of this disease is a mutation in the *RB1* gene, the formed cancerous mass in different patients is seen in non-invasive states, limited to the ocular cavity or in invasive states distributed to other parts of the body. Because this tumor's aggressiveness cannot be predicted early, these patients receive systemic chemotherapy with multiple drugs. Treating non-invasive and invasive tumors separately reduces chemical drug side effects. The aim of this study was to identify diagnostic biomarkers by separating miRNAs in blood serum from invasive and non-invasive RB patients.

Materials and Methods: In this experimental study, selected three gene expression omnibus (GEO) datasets. Two were related to serum and tumor tissue miRNAs, and one was related to non-invasive and invasive *RB* gene expression. Examined *RB* gene-miRNA relationships. Then, we performed real-time polymerase chain reaction (PCR) on candidate miRNAs in the Y79 cell line and patient blood samples in non-invasive and invasive retinoblastoma.

Results: Fourteen high-expression and 7 low-expression miRNAs resulted. *MiR-181, miR-135a, miR-20a, miR-373,* and *miR-191* were common genes with differential genes between invasive and non-invasive retinoblastoma. Only *MiR-181* was upregulated in the Y79 RB cell line. Other candidate miRNAs expressed less. Invasive retinoblastomas increased serum *miR-20a* and *miR-191*.

Conclusion: Integrated and regular bioinformatics analyses found important miRNAs in patients' and *miR-20a, miR-191*, and *miR-135a* can distinguish non-invasive and invasive retinoblastoma, suggesting further research.

Keywords: Gene Expression Profiles, miRNAs, Non-invasive and Invasive, Retinoblastoma

Introduction

Retinoblastoma (RB) is the most prevalent intraocular cancer affecting infants and children, primarily caused by mutations in the tumor suppressor gene *RB1*, thereby categorizing it as a genetically driven cancer (1, 2). The variability in tumor growth rates and invasion patterns among individuals with RB underscores the complexity of its molecular biology and the challenges in prognostication (1). Clinical signs such as leukocoria, strabismus, and glaucoma serve as indicators for RB, with mortality rates ranging from 40-70%, especially in Asia and Africa, often attributed to diagnostic delays and inadequate follow-up (2).

In accordance with international classification standards, RB tumors are categorized into five groups, spanning from less severe cases (seen in non-invasive conditions) such as group A, which involves small tumors situated distantly from the fovea and optic disc, measuring less than 3 mm in diameter, to more critical instances (observed in invasive conditions) like group E, which denotes an expansive tumor spreading across over 50% of the eye globe and infiltrating structures such as the post-laminar optic nerve, choroid, sclera, orbit, and anterior chamber. Accurate classification and staging of RB are crucial for guiding treatment decisions and predicting outcomes (3, 4). Therapeutic approaches typically involve focal therapy or systemic chemotherapy, which may lead to adverse effects such as retinopathies and cataracts (3). Despite advances in diagnostic technologies, predicting

Royan Institute
Cell Journal (Yakhteh)

tumor progression remains challenging, highlighting the need for robust prognostic markers (2, 5). Recent studies have identified RB as a heterogeneous disease, with subtypes exhibiting different aggressiveness rates, thus necessitating the exploration of potential biomarkers (1).

Bioinformatics research in RB has employed various techniques, including gene expression analysis and miRNA profiling, with miRNAs emerging as promising targets for early detection and molecular therapy (6, 7). Alterations in miRNA expression, arising from genetic and epigenetic changes, have been implicated in cancer development, with potential roles as both tumor suppressors and oncogenes (8, 9). Serum and plasma miRNA profiles have been explored as non-invasive diagnostic markers, offering insights into tumor behavior and therapeutic potential (10).

Notably, miRNA signatures in tumor tissue and serum have been associated with clinical and biological changes in tumors, including aggression, response to therapy, and prognosis (10-13). In this study, we investigated differential miRNA expression as potential prognostic biomarkers in aggressive RB compared to low-risk RB, with validation in vitro using an RB cell line.

Materials and Methods

Profiling datasets for gene expression

In this experimental study, the microarray data was obtained from the gene expression omnibus (GEO) database (https://www.ncbi.nlm.nih.gov/geo) with GEO accession number GSE97508. This dataset contained nine samples divided into three groups of three each: non-invasive, invasive RB from RB patients' tissue, as well as cadaveric normal samples. Patients with RB ranged in age from 2 months to 2 years while normal were an average age of 17, 12, and 26 years.

The GEO2R software available in the GEO database was used to identify genes with expression differences between the samples. This software used the GEO query and limma packages as well as R programming, to compare two groups of samples and determine the genes with expression differences between the two groups. The selection criteria for genes included two factors: an adj. $P<0.01$ and ($|logFC|>+1$ for up-regulated genes and $|logFC| <-1$ for down-regulated genes). Data illustrated in Figure S1 (See Supplementary Online Information at www.celljournal.org).

Pathways enrichment analyses

For pathways enrichment analyses, we employed Enrichr (accessible at https://amp.pharm.mssm.edu/Enrichr) in conjunction with the KEGG database (available at https://www.genome.jp/kegg). This allowed us to discern pertinent signaling pathways and the interconnected genes associated with both upregulated and downregulated genes. It's worth mentioning that for the examination of signaling pathways, a P value threshold of 0.05 was utilized in this study.

GO analysis of the genes associated with retinoblastoma

The DEGs were derived from the signaling pathways associated with retinoblastoma and were subjected to analysis across three categories: cellular components, biological processes, and molecular functions. This analysis was carried out using the Database for Annotation, Visualization, and Integrated Discovery (DAVID, available at http://david.ncifcrf.gov), as well as the Panther database (accessible at http://www.pantherdb.org).

Given the identification of pertinent biomarkers, particularly within the category of cellular components, this study placed greater emphasis on the assessment of upregulated genes. Subsequent analyses were then performed on the ten genes exhibiting the highest and lowest levels of expression. In this context, the most relevant gene ontology was determined using a significant threshold of a $P<0.05$.

Conducted research into the interaction of proteins

The protein network was assembled by inputting the chosen genes into the STRINGS database (accessible at https://string-db.org). For enhanced data visualization, we employed Cytoescape version 3.7.1.

Datasets containing the profiles of microRNA expressions

For this section of our experimental study, two retinoblastoma patient datasets were chosen. The GSE41321 dataset examined miRNAs in serum, while the GSE7072 dataset focused on miRNAs in tissue. Each dataset comprised six samples, with three obtained from retinoblastoma patients and three from healthy blood or tissue samples. We identified differentially expressed miRNAs by using GEO2R. The miRNA expression profiles were segregated, and a $P=0.05$ was computed. Subsequently, miRNAs with both high and low expression levels were separately clustered in Venn diagrams for the serum and tissue datasets. This process facilitated the identification and classification of common miRNAs.

Candidate miRNAs

In this section of the study, the Enrichr database was utilized to upload the most relevant genes associated with retinoblastoma. Subsequently, the TargetScan database (accessible at http://www.targetscan.org) was employed to analyze and categorize the crucial miRNAs that connect with these genes. The selection of miRNAs was contingent on a significance threshold of a $P<0.05$.

Two distinct methodologies were employed to explore this aspect of the investigation. Initially, we compared the miRNAs that exhibited up- and down-regulation in both serum and tissue samples. Next, we examined the most frequently reported miRNAs in the existing literature. Following this, we inputted the chosen miRNAs into the TargetScan database, retrieved their target genes, and cross-referenced them with the genes from the initial dataset GSE7072. Leveraging previously published data, we scrutinized the miRNA expression profiles

and categories (non-invasive retinoblastoma, invasive retinoblastoma from tissue of retinoblastoma patients, and normal samples obtained from cadavers) in both the serum and tissue samples.

Cell culture

Y79 retinoblastoma cells, sourced from the Royan Cell Bank, were cultured using RPMI 1640 medium. This culture medium was supplemented with 10% (v/v) heated-inactivated fetal bovine serum (FBS), 100 IU/ml of penicillin, 100 mg of streptomycin, and 2 mM of L-glutamine (all from Gibco, USA). The cell-containing culture, passage between 40-45, was maintained in an environment with 5% CO_2 at a temperature of 37°C, within a humidified atmosphere, to facilitate future research endeavors. All procedures involving the human cell and tissue were approved by Royan Institute Committee for Ethics in Research.

Human retinal tissue was required for this experiment

The donors of the retinal tissue were from Iran eye bank, two men and a woman, met the criteria for selection as they suffered brain death due to a car accident at the respective ages of 27, 32, and 38. It was essential that the individuals chosen for this study were between the ages of 20 and 40 and did not have any pre-existing conditions affecting their kidneys, liver, metabolism, or vision.

At the Iran eye bank, the retinas from the three eyes of the donors were carefully extracted and promptly frozen in liquid nitrogen. This was accomplished by immersing the samples in liquid nitrogen for a duration of two minutes, after which they were placed in RNase vials and submerged once again in liquid nitrogen. Subsequently, the samples were transported to the research institute and stored in a -80°C freezer until real-time PCR tests could be conducted.

Real-time polymerase chain reaction

For this phase, we procured the BON-miR miRNA 1st-Strand cDNA Synthesis (BON209001) and BON-miR miRNA High-Specificity QPCR Core Reagent (BON209002) kits from the Stem Cell Technology Company. Following the provided instructions, we performed cDNA synthesis and quantitative real-time PCR (QRT-PCR). The tubes containing the reaction mixtures were securely sealed and then placed in a thermocycler set at 75°C for 5 minutes. After this, the tubes were promptly cooled, and the necessary components were added.

We meticulously prepared the desired composition in the thermocycler following the protocol provided with the BON-miR QPCR kit. This kit conveniently includes all the essential components required for a real-time reaction on miRNA-prepared cDNA. The cDNAs from the previous step underwent a qRT-PCR reaction utilizing the compounds and adhering to the program's

instructions. All of these steps were executed in a dimly lit, light-protected environment. Finally, we loaded the tubes with the necessary materials and placed them in the thermocycler for the specified duration.

Patients' blood samples

In collaboration with Torfeh and Rasoul Akram Hospitals in Tehran, blood samples were collected from patients with coagulated blood, extracting two to four milliliters via centrifugation. The patients were then categorized into two groups: invasive procedures and non-invasive according to clinical features. Additionally, factors such as inheritance, disease recurrence, symmetry, and disease stage were taken into consideration. Upon arrival at the research institute, the blood samples were promptly placed on ice and subsequently centrifuged in tubes at 4,000 revolutions per minute for a duration of 20 minutes. Following centrifugation, the serum was carefully extracted and then stored in a free RNase tube at -80°C, awaiting PCR analysis. Details about the patient and control populations from whom blood samples were obtained can be found in Table S1 (See Supplementary Online Information at www.celljournal.org).

Examination of statistical data

Bioinformatics data was consistently assessed and integrated into this study utilizing the prescribed methods. Specifically, for cell line samples, the t test, a non-parametric statistical test, was employed. On the other hand, for blood samples, an Analysis of Variance (ANOVA) was utilized. The statistical software GraphPad Prism version 9 was employed for data analysis. Significance was attributed to outcomes with a $P<0.05$.

Results

Higher gene expression related to tumor formation and the visual cycle in invasive retinoblastoma compared to non-invasive retinoblastoma

According to the GSE97508 dataset, it was observed that 127 genes showed an increase in expression while 184 genes exhibited a decrease in expression in the invasive group compared to the non-invasive group. This suggests that these genes that displayed an increase in expression in the invasive group might play a role in the development and progression of retinoblastoma. Additionally, CAMs, TNF signaling, ECM-receptor interaction, and primary immunodeficiency pathways were upregulated. On the other hand, oxidative phosphorylation, the spliceosome, DNA replication, HIF-1 signaling, the cell cycle, and AMPK signaling pathways were downregulated. In terms of specific genes, *GUCA1C*, *ARR3*, and *WIF1* demonstrated the lowest expression levels, whereas *POM121L8P*, *PCMTD2*, and *SPTLC3* exhibited the highest levels of expression (Fig.1).
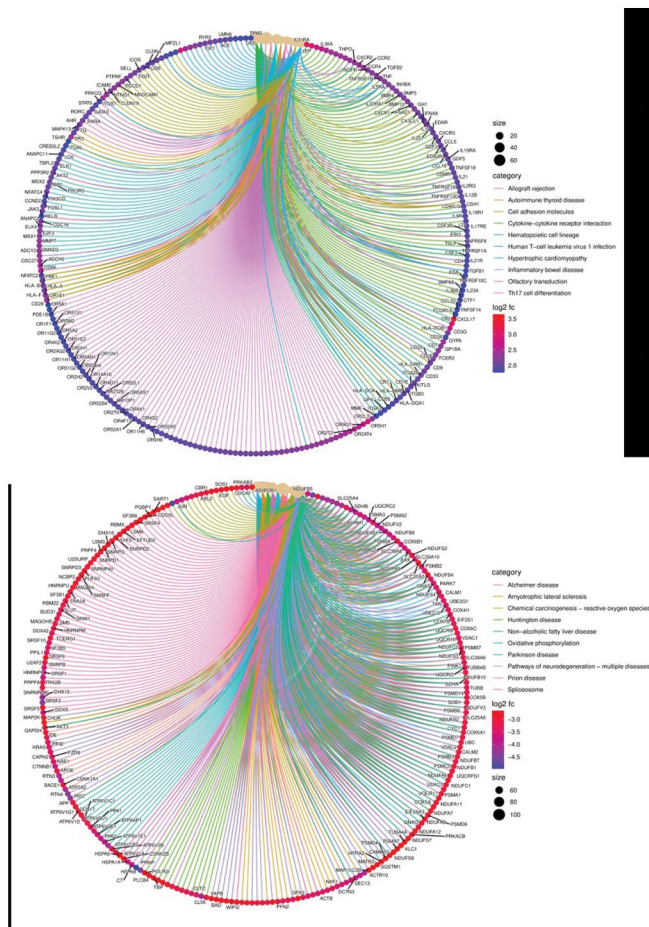
252

Fig.1: Genes with differential expression between the invasive and non-invasive groups of retinoblastomas are identified. The signaling pathways of the upregulated and downregulated genes involved in retinoblastoma have been shown.

Gene ontology between noninvasive and invasive retinoblastoma

In this segment from the results of the Enrichr and KEGG database, we analyzed genes that were either upregulated or downregulated across three categories: biological processes, molecular functions, and cellular components. Biological processes exhibited activities such as extracellular matrix organization, signaling pathways mediated by cytokines, positive regulation of cell proliferation, control of apoptotic processes, and positive regulation of cell migration. Regarding cellular components, the extracellular matrix showed notably increased levels of activities including phosphatidylinositol 3-kinase activity, frizzled binding, integrin binding, vascular endothelial growth factor receptor 2 binding, and cytokine activity. In terms of biological processes, RNA splicing was identified through transesterification reactions using bulged adenosine as the nucleophile, along with the respiratory electron transport chain, the cell cycle G1/S phase transition, and insulin receptor signaling pathways. Conversely, for downregulated genes, activities such as NADH dehydrogenase (ubiquinone) activity, pre-mRNA binding, and ATPase activity were implicated in molecular functions (Fig.S2, See Supplementary Online Information at www.celljournal.org, Table 1).

An examination of the protein network

The second section of the study focused on genes linked to up-regulated pathways. This network, comprising 95 nodes and 514 edges, illustrates the connection between proteins associated with eye development, camera-type eye development, TNF signaling, ECM-receptor interaction, PI3K-Akt signaling, axon guidance, and GABAergic synapse pathways (Fig.S3, See Supplementary Online Information at www.celljournal.org).

In serum and retinoblastoma tissue, DEG-miRNAs were identified

Serum and tissue samples underwent analysis to detect up- and downregulated miRNAs. The overlapping miRNAs were then assessed using a Venn diagram, revealing miR-302d, miR-135b, miR-412, miR-194, miR-144, miR-340, miR-132, miR-141, and miR-142-3p. These miRNAs target various genes, including cell adhesion molecules, TNF signaling, T cell receptor, MAPK signaling, VEGF signaling, Ras signaling, Proteoglycan in cancer, and AMPK signaling. Additionally, serum samples from retinoblastoma patients exhibited reduced expression of miR-204 (Figs.2, 3, Table 2).
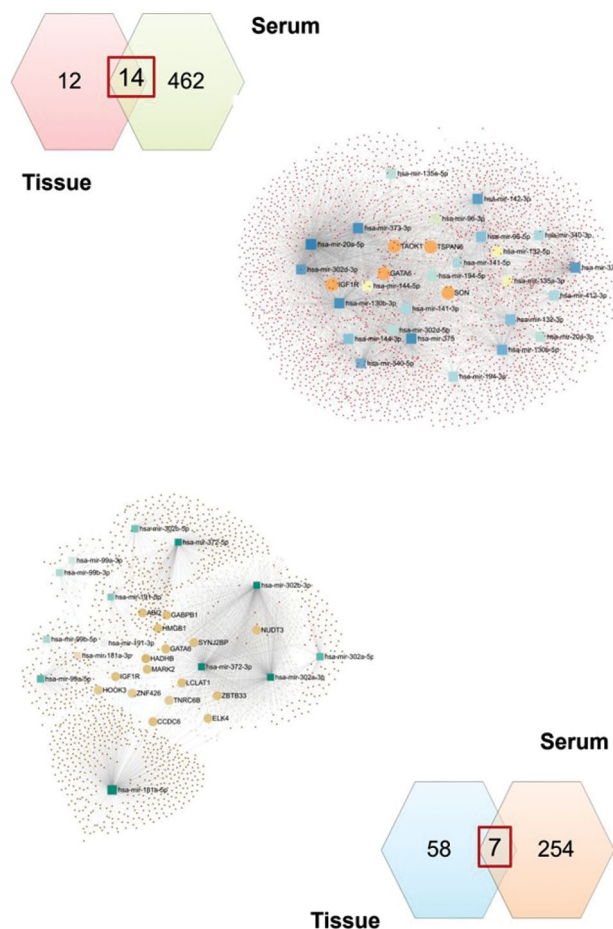

Fig.2: Network of communication between serum and tissue miRNAs of patients with retinoblastoma. Subscriptions were first made using the Venn diagram, and then the link between miRNAs and their target genes was plotted.

Table 1: Molecular functions in up- and down-regulated genes between invasive and non-invasive of retinoblastoma

|	Term	P value	Genes
Up- regulated	Phosphatidylinositol 3-kinase activity	1.61E-12	*CD86, KITLG, FGF20, CD28, PIK3CD, PIK3R3, FGF1, ICOS, EGFR, FGFR2, PIK3R5*
	Phosphatidylinositol-4,5-bisphosphate 3-kinase activity	1.46E-11	*CD86, KITLG, FGF20, CD28, PIK3CD, FGF1, ICOS, EGFR, FGFR2, PIK3R5*
	Phosphatidylinositol bisphosphate kinase activity	2.29E-11	*CD86, KITLG, FGF20, CD28, PIK3CD, FGF1, ICOS, EGFR, FGFR2, PIK3R5*
	G-protein coupled receptor binding	1.2E-08	*ARHGEF11, WNT10B, ITGB4, FZD7, CCL5, WNT5A, WNT8A, WNT1, WNT4, GNAI2*
	Cytokine activity	5.21E-08	*BMP4, EDN1, TGFB1, CSF1, TGFB3, CCL5, WNT1, TNF, CX3CL1, VEGFA*
	Frizzled binding	1.1E-07	*WNT10B, FZD7, WNT5A, WNT8A, WNT1, WNT4*
	Integrin binding	1.4E-07	*VTN, ITGB3, ICAM2, ICAM3, MADCAM1, IGF1, FGF1, CX3CL1*
	1-phosphatidylinositol-3-kinase activity	7.28E-06	*FGF20, PIK3CD, PIK3R3, FGF1, FGFR2*
	Protease binding	9.84E-06	*COL1A1, SELL, ITGA3, ITGB3, CD28, BCL2, TNF*
Down- regulated	NADH dehydrogenase	4.74E-26	*NDUFB9, NDUFA13, NDUFA7, NDUFB7, NDUFB6, NDUFB10, NDUFA12, NDUFB5, NDUFA4, NDUFB4, NDUFA1, NDUFC2, NDUFS7, NDUFAB1, NDUFS4, NDUFS2, NDUFV3, NDUFV2*
	ATPase activity, coupled to transmembrane movement of ions, rotational mechanism	4.83E-25	*ATP6V1A, ATP6V0B, ATP6V0E1, ATP5A1, ATP5G3, ATP5H, ATP5G2, ATP5F1, ATP5G1, ATP5L, ATP5B, ATP5D, ATP6V1B2, ATP6V0D1, ATP6V1C1*
	Hydrogen ion transmembrane transporter activity	1.28E-22	*ATP6V1A, ATP6V0B, ATP6V0E1, UQCRB, ATP5A1, ATP5G3, UQCR10, ATP5H, ATP5G2, ATP5F1, ATP5G1, ATP5L, ATP5B, ATP5D, ATP6V1B2, ATP6V0D1, ATP6V1C1*
	RNA binding	6.86E-19	*TCERG1, EIF4A3, DDX42, ATP5C1, ENO1, ELAVL1, SART1, SNRPD2, SNRPD1, MAGOH, DHX15, DHX16, NCBP2. YWHAZ, SYF2, PRPF3, SRSF2, SNRPG, SRSF3, SRSF4, SRSF5, SNRPF, SRSF6, SNRNP200, SNRPB, RBM22, DDX5, SF3B3, PRKDC, ATP5A1, SRSF1, PRPF8, PUF60, TRA2B, TRA2A, NDUFV3, HNRNPA1, PPARGC1A, EIF4E, SMAD2, HSPA8, LSM5, MAGOHB, EEF2, LSM3, HNRNPM, SNRNP40, HNRNPK, SNW1, SSBP1, RBMX, HSPA1A*
	Proton-transporting ATP synthase activity, rotational mechanism	2.10E-17	*ATP5B, ATP5D, ATP5A1, ATP5H, ATP5G3, ATP5F1, ATP5G2, ATP5G1, ATP5L*
	Cation-transporting ATPase activity	3.31E-12	*ATP5B, ATP5A1, ATP5D, ATP5G3, ATP5H, ATP5G2, ATP5F1, ATP5G1, ATP5L*
	Proton-transporting ATPase activity, rotational mechanism	5.31E-11	*ATP6V1A, ATP5B, ATP6V0B, ATP6V0E1, ATP6V1B2, ATP6V0D1, ATP6V1C1*
	Hydrogen-exporting ATPase activity	5.19E-10	*ATP6V1A, ATP5B, ATP6V0B, ATP6V0E1, ATP6V1B2, ATP6V0D1, ATP6V1C1*

A

B

C

D
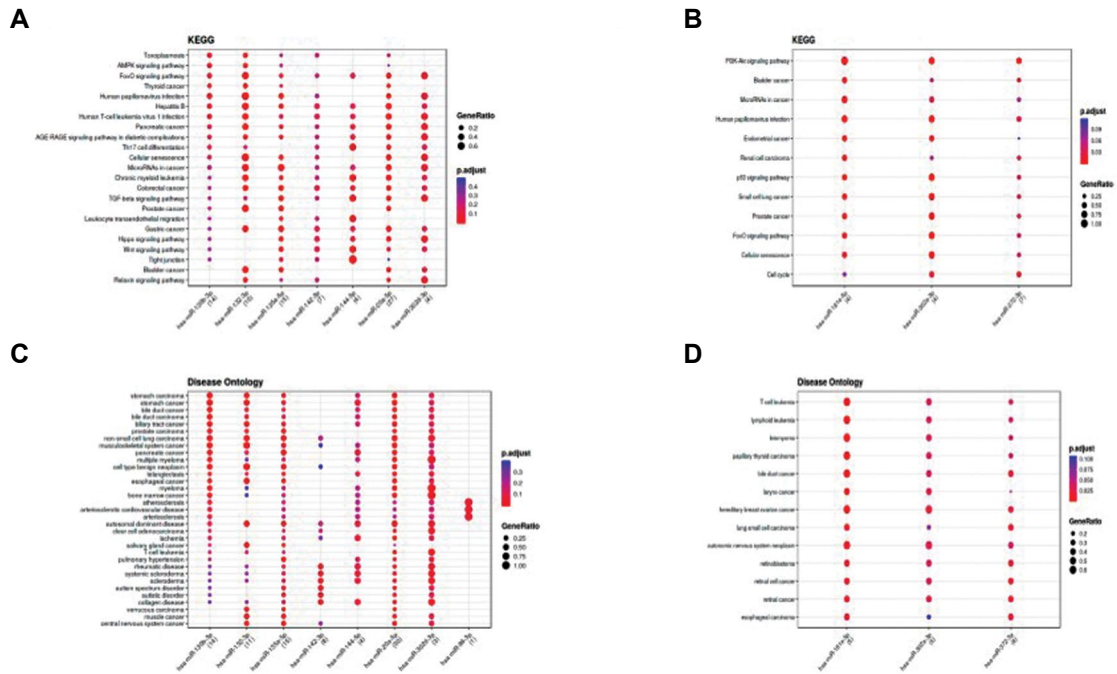
Fig.3: The role of common miRNAs between serum and tissue of patients with retinoblastoma has been demonstrated based on the signal pathway and their presence in various diseases. The color of the circles is significantly related, and the size of the circles is related to the number of target genes.

Table 2: List of intersection upregulated miRNAs between serum and tissue

Expression pattern	Name upregulated miRs	Log FC serum	Log FC tissue	P value serum	P value tissue
Up-regulated	hsa-miR-302d	6.9142733	1.904316	0.00966694	0.04302966
	hsa-miR-135a	4.426793	2.72321	0.04929709	0.03371782
	hsa-miR-412	4.2122315	1.906788	0.03936273	0.037093
	hsa-miR-194	3.0699777	2.071652	0.00031874	0.04901003
	hsa-miR-375	3.1616598	2.301253	0.00715124	0.0414571
	hsa-miR-144	2.0055241	2.584919	0.00378621	0.0136798
	hsa-miR-340	2.2239905	2.550753	0.00264811	0.0218318
	hsa-miR-132	2.2696722	2.09459	0.02048582	0.04726511
	hsa-miR-141	2.391614	1.693513	0.04315546	0.01962257
	hsa-miR-142-3p	1.2252598	2.326177	0.01330823	0.02249177
	hsa-miR-96	1.2375568	1.995808	0.01909967	0.04440636
	hsa-miR-130b	1.2537009	2.476639	0.00942933	0.01898687
	hsa-miR-373	6.6023058	3.47031	0.00310248	0.00250759
	hsa-miR-20a	4.2836682	1.73307	0.00666911	0.01489773
Down- regulated	hsa-miR-99b	-1.5749361	-3.342798	0.02000544	0.03430489
	hsa-miR-181a*	-2.28297	-3.015084	0.02208	0.01355216
	hsa-miR-191	-2.40289	-2.846559	0.02393922	0.00095681
	hsa-miR-302b*	-2.5153418	-2.067435	0.02858573	0.04487058
	hsa-miR-99a	-2.999783	-2.407591	0.01654146	0.0107814
	hsa-miR-302a	-3.8771579	-2.192216	0.00816953	0.00656692
	hsa-miR-372	-5.2840495	-2.001038	0.02592317	0.01851424

*; Following a miRNA identifier, denotes the less predominant mature sequence derived from the 3' arm of the precursor hairpin.

miRNA expression profiling in Y79 cell line and blood samples

In this phase of the research, we utilized data from the bioinformatics analysis section to evaluate miRNA expression in the cell line. As depicted in Figure 4, miR-181 exhibited notably elevated levels in the Y79 cell line, when compared to human normal retinal tissue. On the other hand, other miRNAs, such as miR-373, miR-20a, miR-191, and miR-135a, demonstrated lower expression levels in the cell line compared to healthy retinal tissue (Fig.4A). Additionally, we assessed the expression of specific miRNAs in blood samples obtained from both invasive and non-invasive retinoblastoma patients as well as healthy individuals. In Figure 4B, it is evident that miR-20a exhibited significantly higher expression in invasive retinoblastoma compared to non-invasive cases. In addition, miR-191 showed that its expression was higher in invasive retinoblastoma than in non-invasive retinoblastoma.
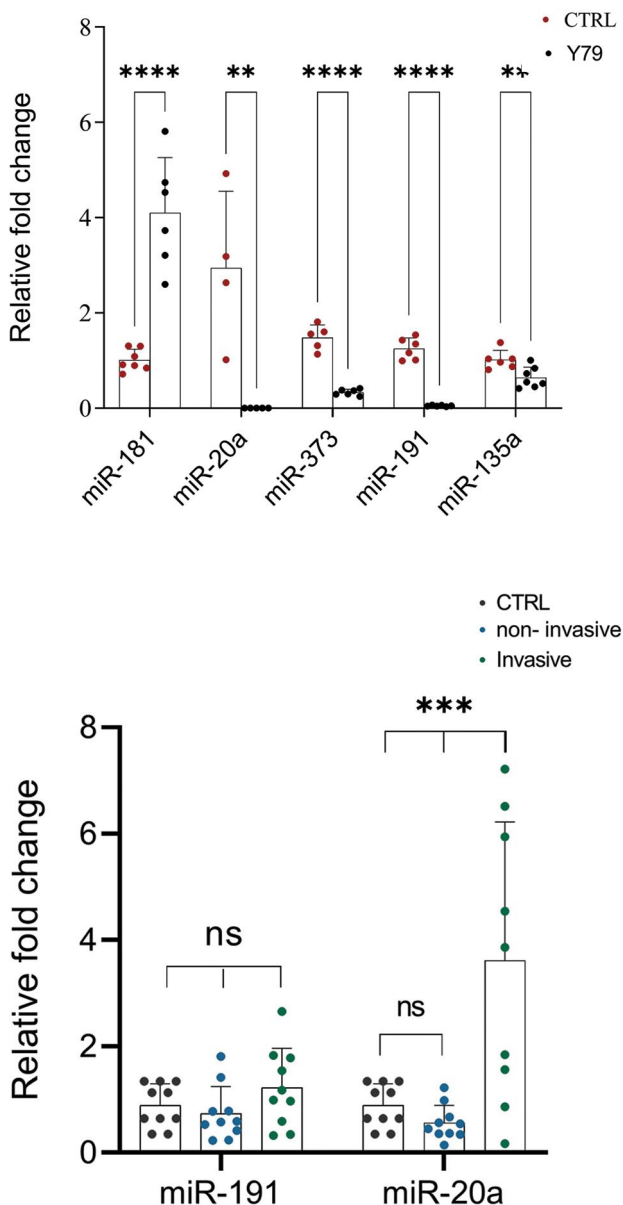

Fig.4: Real-time analysis of microRNAs between Y79 cell line and healthy retinal tissues.

Discussion

RB can be catastrophic for infants and neonates if not discovered early. Many studies have been done to find RB biomarkers. Molecular markers have been established to detect this malignancy early (14, 15). In this study, researchers employed continuous and integrated bioinformatics to examine the connection between genes implicated in non-invasive and invasive *RB* gene expression profiles and other types of cancers. We chose proteins and genes from these two groups to predict illness severity. We chose miRNAs based on their expression profiles and similarities across blood and tissue samples. These studies first examined the Y79 cell line, then patient blood samples.

Initial bioinformatics research of non-invasive and invasive *RB* gene expression patterns showed cell adhesion pathways, extracellular matrix, TNF, and the visual cycle. Adhesion molecules are needed for cell structure, division, and migration (16). Inhibiting this pathway and related genes and proteins may speed cancer cell spread. In research of 35 RB tissues and 8 normal retinal tissues, RB tissue produced higher amounts of CD-44 and MMP-14 proteins. Ki-67's two discovered proteins were further studied to better understand their role in cell division. Each marker was more numerous in RB tissue than in a control sample. Extracellular matrix cell adhesion molecules are needed for replenishing extracellular space and inhibiting cancer cell migration. Numerous investigations have been undertaken on extracellular matrix and RB functional genes and proteins. Proteomic experiments created extracellular vesicles. Eye tumor particles were examined more closely. On this premise, gene function and protein activity in the cell or extracellular environment were examined. SNAP25, MPDZ, AK2, CKB, EIF1, PPP2R1B, and other proteins implicated in RB cell invasion were detected in the cell and extracellular matrix. RB worsens it (17). Invasion and migration of RB cells require MMP-2 and MMP-9, according to another study. ShRNAs reduced RB cancer cell survival and boosted apoptosis by inhibiting two proteins. MMP-2 and MMP-9 prevent RB cell invasion (18). Another study linked FOXM1 and MMP-2 expression and activity.

A transcriptome and kinome analysis of eight RB tissue samples revealed that GUCA1C, GABRR2, PDC, PDE6C, EYS, MYO3B, and KIFC3 distinguish unilateral from bilateral RB (19). Another study evaluated the expression profiles of proteins in RB patients and healthy controls (20). Deacetylating histones and reducing UHRF1 expression, a ubiquitination component, had anticancer effects in retinoblastoma. Factors affect oxidative stress and apoptosis. Reduced UHRF1 activity enhances GUCA1C expression, which improves RB patients' visual cycle (21).

This study compared miRNAs from non-invasive and invasive RB tissue and blood samples. *hsa-miR-302d, hsa-miR-135b, hsa-miR-412, hsa-miR-375, hsa-miR-144, hsa-miR-340,* and *hsa-miR-132* MiRNAs and

their target genes are linked to aggressive non-invasive retinoblastoma. Cell lines and testing samples have *hsa-miR-191*, *hsa-miR-135a*, *hsa-miR-181*, and *hsa-miR-373*.

Researchers compared serum and RB tumor tissue for common miRNAs to find tumor-specific miRNAs released into the bloodstream. Due to the high number of miRNAs in blood, miRNAs associated with RB tumors can be identified and exploited as targeted treatments.

Numerous investigations on RB found strong expression of hsa-*miR-181*. They employed TaqMan MicroRNA Assays to investigate the miRNA profiles of two RB cell lines (Y79, WERI-Rb1) and two 12-week-old fetal retinae. When normalized against *hsa-let7a*, five miRNAs were up-regulated (4-60-fold) in retinal tissues and cell lines (22). *hsa-miR-93, hsa-miR-181*, and *hsa-miR-183* were also present and up-regulated. These miRNAs are significantly expressed in mouse retina (23).

Also explored is *hsa-miR-191*, *hsa-miR-373*, *hsa-let-7b*, and other miRNA molecules target genes involved in the cell cycle process, according to Yang et al. (23) *hsa-miR-373*, *hsa-miR-125b*, *hsa-miR-18a*, *hsa-miR-25*, *hsa-miR-191*, *hsa-let-7*, *hsa-miR-25*, *hsa-miR-18a*, and *hsa-miR-20a* targeted BCL2L11, CDC25A, CDK6, and LIN28. The miRNA-target regulatory network identifies miRNA targets for medication development and therapy. MDM4 is a p53 antagonist in RB and developing retina. Retinal MDM4 levels are greater than in embryonic retinae. MiR191 was downregulated in RB relative to embryonic retinas. Somatic mutations in retina xenografts removed miR-191 binding sites (24). X-inactive specific transcript (XIST) is an oncogenic lncRNA. Xu et al. (25) employed qRT-PCR or Western blot to measure XIST, *miR-191-5p*, BDNF mRNA, and BDNF in RB cells. Overexpression of XIST enhanced RB cell proliferation, migration, invasion, and death, while miR-191 reduced growth and proliferation. XIST indirectly increased BDNF gene expression by decreasing luciferase reporter assays and endogenous RNA.

hsa-miR-135a activity and expression have been seen in malignancies. According to a study, reduced *miR-135a* expression in NSCLC patients' serum was associated with a poor prognosis and shorter 3-year overall survival. *miR-135a* overexpression and ROCK1 suppression can decrease malignant cell growth and diffusion and enhance apoptosis and Bax, Caspase3, and E-cadherin expression. Transfected HCC827, NCI-H524 cells and mice showed malignant growth and diffusion like non-transfected cells (26). More DANCR knockdown decreased TSCC cell survival and hindered migration and invasion *in vitro*, while ectopic expression had the opposite impact. *In vivo*, DANCR reduced tumor development and MMP-2/9 and KLF8 expression. *miR-135a* suppressed DANCR and reversed its positive effects on TSCC tumors (26). *In vitro* and *in vivo*, *miR-135a* boosted growth, proliferation, and invasion of an HPV-16 E6/E7-immortalized cervical epithelial cell line, NC104-E6/E7. The observed effects were due to SIAH1's inhibitory influence on –beta

catenin cell factor signaling. MiRNA overexpression enhanced cervical cancer cell proliferation in low-density culture, which SIAH1 partially reversed. Malignant cervical squamous cell carcinoma overexpresses miRNA compared to precancerous lesions (27). Trans well assays show that *miR135a* reduces U251 cell growth and invasion. FOXO1 is a *miR-135a* target and may reverse its actions in glioma patients. *miR-135a* expression was downregulated in gliomas, while FOXO1 expression was upregulated (28). Immunohistochemistry and qRT-PCR showed decreased *miR-135a-5p* expression in gallbladder cancer (GBC) tissue. Angiopoietin 2 (ANGPT2) is the GBC *miR-135a-5p* target gene. Downregulating ANGPT2 inhibited GBCSD cell growth and invasion. Androgen-induced *miR-135a* inhibits prostate cancer cell growth, migration, cell cycle arrest, and apoptosis (29). RBAK and MMP11 were identified using bioinformatics and experiments. *miR-135a* may be downregulated by androgen depletion and/or PI3K/AKT hyperactivation in castration-resistant prostate cancer (30). In this work, the expression level in the cell line was much lower than in healthy retinal tissue. RB can be studied utilizing a variety of experimental approaches.

Finally, determining whether a child has aggressive or non-invasive RB at the time of their initial visit to a medical center can be critical in-patient management and preventing them from enucleation their eyes. *miR-20a*, *miR-135a*, and *miR-191* were identified in this study as potential biomarkers for invasive versus non-invasive RB and will be further investigated.

Acknowledgements

Authors' Contributions

A.B.; Collection, Data analysis, Interpretation, and Manuscript writing. M.S.M.; Contributed to investigation. S.K., A.-A.H.A., M.F.; Provided retinoblastoma blood samples, Advising, Read, and Edit the revise version of manuscript. S.T., L.S.; Conducting experiments, Conception, Design, Data analysis, Interpretation, Administrative, and Financial support. All authors read and approved this final manuscript.

References

1. Parveen S, Sahoo SK. Evaluation of cytotoxicity and mechanism of apoptosis of doxorubicin using folate-decorated chitosan nanoparticles for targeted delivery to retinoblastoma. Cancer Nanotechnol. 2010; 1(1-6): 47-62.
2. Liu H, Cao B, Zhao Y, Liang H, Liu X. Upregulated miR-221/222 promotes cell proliferation and invasion and is associated with invasive features in retinoblastoma. Cancer Biomark. 2018; 22(4): 621-629.
3. Danda R, Ganapathy K, Sathe G, Madugundu AK, Krishnan UM, Khetan V, et al. Membrane proteome of invasive retinoblastoma: differential proteins and biomarkers. Proteomics Clin Appl. 2018; 12(5): e1700101.
4. Gerrish A, Bowns B, Mashayamombe-Wolfgarten C, Young E, Court S, Bott J, et al. Non-Invasive prenatal diagnosis of retino-

blastoma inheritance by combined targeted sequencing strategies. J Clin Med. 2020; 9(11): 3517.

5. Lu JE, Francis JH, Dunkel IJ, Shields CL, Yu MD, Berry JL, et al. Metastases and death rates after primary enucleation of unilateral retinoblastoma in the USA 2007-2017. Br J Ophthalmol. 2019; 103(9): 1272-1277.

6. Shields CL, Bas Z, Laiton A, Silva AMV, Sheikh A, Lally SE, et al. Retinoblastoma: emerging concepts in genetics, global disease burden, chemotherapy outcomes, and psychological impact. Eye (Lond). 2023; 37(5): 815-822.

7. Garcia JR, Gombos DS, Prospero CM, Ganapathy A, Penland RL, Chévez-Barrios P. Expression of angiogenic factors in invasive retinoblastoma tumors is associated with increase in tumor cells expressing stem cell marker Sox2. Arch Pathol Lab Med. 2015; 139(12): 1531-1538.

8. Fabian ID, Reddy A, Sagoo MS. Classification and staging of retinoblastoma. Community Eye Health. 2018; 31(101): 11-13.

9. Mendoza PR, Grossniklaus HE. Therapeutic options for retinoblastoma. Cancer Control. 2016; 23(2): 99-109.

10. Chantada G, Schaiquevich P. Management of retinoblastoma in children: current status. Paediatr Drugs. 2015; 17(3): 185-198.

11. Wang X, Kaczor-Urbanowicz KE, Wong DT. Salivary biomarkers in cancer detection. Med Oncol. 2017; 34(1): 7.

12. Sun J, Xi HY, Shao Q, Liu QH. Biomarkers in retinoblastoma. Int J Ophthalmol. 2020; 13(2): 325-341.

13. Cao M, Wang S, Zou J, Wang W. Bioinformatics analyses of retinoblastoma reveal the retinoblastoma progression subtypes. PeerJ. 2020; 8: e8873.

14. Wu D, Rice CM, Wang X. Cancer bioinformatics: a new approach to systems clinical medicine. BMC Bioinformatics. 2012; 13: 71.

15. Hao F, Mou Y, Zhang L, Wang S, Yang Y. LncRNA AFAP1-AS1 is a prognostic biomarker and serves as oncogenic role in retinoblastoma. Biosci Rep. 2018; 38(3): BSR20180384.

16. Najafi M, Farhood B, Mortezaee K. Extracellular matrix (ECM) stiffness and degradation as cancer drivers. J Cell Biochem. 2019; 120(3): 2782-2790.

17. Galardi A, Colletti M, Lavarello C, Di Paolo V, Mascio P, Russo I, et al. Proteomic profiling of retinoblastoma-derived exosomes reveals potential biomarkers of vitreous seeding. Cancers (Basel). 2020; 12(6): 1555.

18. Morales-Cámara S, Alexandre-Moreno S, Bonet-Fernández JM, Atienzar-Aroca R, Aroca-Aguilar JD, Ferre-Fernández JJ, et al. Role of GUCA1C in primary congenital glaucoma and in the retina: functional evaluation in zebrafish. Genes (Basel). 2020; 11(5): 550.

19. Alvarez-Suarez DE, Tovar H, Hernández-Lemus E, Orjuela M, Sadowinski-Pine S, Cabrera-Muñoz L, et al. Discovery of a transcriptomic core of genes shared in 8 primary retinoblastoma with a novel detection score analysis. J Cancer Res Clin Oncol. 2020; 146(8): 2029-2040.

20. Naru J, Aggarwal R, Mohanty AK, Singh U, Bansal D, Kakkar N, et al. Identification of differentially expressed proteins in retinoblastoma tumors using mass spectrometry-based comparative proteomic approach. J Proteomics. 2017; 159: 77-91.

21. Kim JK, Kan G, Mao Y, Wu Z, Tan X, He H, et al. UHRF1 down-modulation enhances antitumor effects of histone deacetylase inhibitors in retinoblastoma by augmenting oxidative stress-mediated apoptosis. Mol Oncol. 2020; 14(2): 329-346.

22. Chakraborty S, Khare S, Dorairaj SK, Prabhakaran VC, Prakash DR, Kumar A. Identification of genes associated with tumorigenesis of retinoblastoma by microarray analysis. Genomics. 2007; 90(3): 344-353.

23. Yang Y, Mei Q. miRNA signature identification of retinoblastoma and the correlations between differentially expressed miRNAs during retinoblastoma progression. Mol Vis. 2015; 21: 1307-1317.

24. McEvoy J, Ulyanov A, Brennan R, Wu G, Pounds S, Zhang J, et al. Analysis of MDM2 and MDM4 single nucleotide polymorphisms, mRNA splicing and protein expression in retinoblastoma. PLoS One. 2012; 7(8): e42739.

25. Xu Y, Fu Z, Gao X, Wang R, Li Q. Long non-coding RNA XIST promotes retinoblastoma cell proliferation, migration, and invasion by modulating microRNA-191-5p/brain derived neurotrophic factor. Bioengineered. 2021; 12(1): 1587-1598.

26. Zheng Y, Zheng B, Meng X, Yan Y, He J, Liu Y. LncRNA DANCR promotes the proliferation, migration, and invasion of tongue squamous cell carcinoma cells through miR-135a-5p/KLF8 axis. Cancer Cell Int. 2019; 19: 302.

27. Leung CO, Deng W, Ye TM, Ngan HY, Tsao SW, Cheung AN, et al. miR-135a leads to cervical cancer cell transformation through regulation of β-catenin via a SIAH1-dependent ubiquitin proteosomal pathway. Carcinogenesis. 2014; 35(9): 1931-1940.

28. Shi HZ, Wang DN, Xu F, Teng JH, Wang YL. miR-135a inhibits glioma cell proliferation and invasion by directly targeting FOXO1. Eur Rev Med Pharmacol Sci. 2018; 22(13): 4215-4223.

29. Diao H, Xu X, Zhao B, Yang G. miR135a5p inhibits tumor invasion by targeting ANGPT2 in gallbladder cancer. Mol Med Rep. 2021; 24(1): 528.

30. Wan X, Pu H, Huang W, Yang S, Zhang Y, Kong Z, et al. Androgen-induced miR-135a acts as a tumor suppressor through downregulating RBAK and MMP11, and mediates resistance to androgen deprivation therapy. Oncotarget. 2016; 7(32): 51284-51300.